

Design Feature

BOUALEM MANSOURI | Doctor

MEHADJI ABRI | Doctor
Telecommunications Laboratory, Faculty of
Technology, University of Tlemcen, Algeria

MOHAMED AMINE RABAH | Doctor

HADJIRA ABRI | Doctor
STIC Laboratory, Faculty of Technology,
University of Tlemcen, Algeria

JUNWA TAO | Professor

TAN-HOA VUONG | Doctor
LaPlace Laboratory, Ensheeih,
University of Toulouse, France

SIW Bandpass Filter Screens S-Band Signals

Substrate-integrated-waveguide (SIW) technology can be applied toward the design and fabrication of a low-cost, compact S-band bandpass filter.

Substrate-integrated-waveguide (SIW) technology can bring some of the performance benefits of waveguide transmission lines to compact microstrip printed-circuit-board (PCB) components, including filters. To demonstrate some of the promise of SIW technology, a bandpass filter was designed for use at S-band frequencies. By using resonant cavities based on SIW technology, excellent filtering results were achieved in the desired frequency bands. The filter achieved a passband of 2.75 to 3.40 GHz with low passband loss, with close agreement between measured and simulated results.

Expansion of telecom systems in recent years has required the development of high-performance equipment at reasonable prices. This need has impacted systems at all frequencies, including at RF and microwave frequencies. Some low-loss components, such as waveguide filters, have provided good performance—albeit with a tradeoff in size and weight, where some applications were in need of lighter, more compact components. SIW technology is one of the approaches that has provided high-performance component solutions at a fraction of the size and weight of traditional rectangular waveguide components.¹⁻⁴

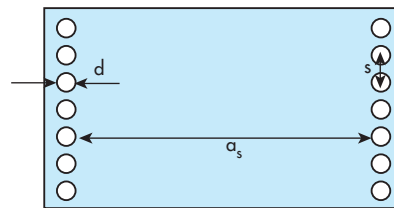
SIW technology combines some of the performance benefits of traditional rectangular waveguide with the compact size of planar transmission lines. The waveguide benefits include low loss, compact size, high quality factor (Q), and the potential for handling high power levels

with low electromagnetic (EM) radiation. SIW approaches allow different components to be designed and constructed as integrated components with one manufacturing process, rather than build them separately and then combine them into a subassembly.

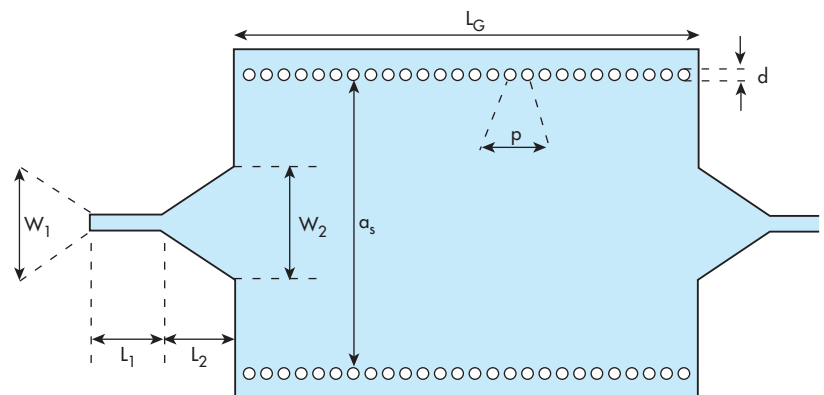
Filters, phase shifters, antennas, and other components can be designed and constructed in SIW rather than in rectangular waveguide. This helps to reduce both the overall dimensions of a telecommunications system and the cost of manufacturing these components. Although SIW technology is still relatively new and not considered

a mature technology, it has been applied to a number of different components and subsystems by different design teams and has shown consistent, stable performance over time and temperature.

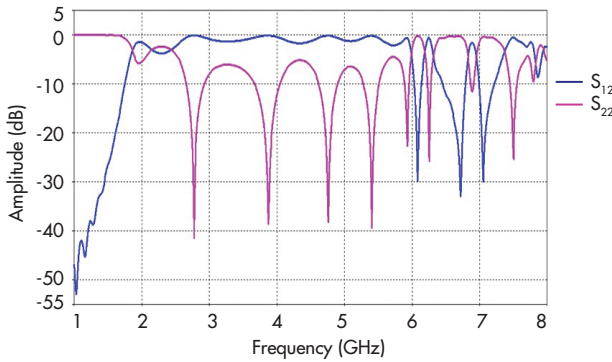
In addition, with time, a growing number of SIW component models become available in commercial computer-aided-



1. This diagram illustrates the SIW topology adopted for the bandpass filter.



2. This is a top view of the SIW filter, with the following parameters: $p = 3$ mm; $L_G = 80$ mm; $d = 2$ mm; $a_s = 51.4$ mm; $W_2 = 19.28$ mm; $W_1 = 2.99$ mm, $L_1 = 12.35$ mm; and $L_2 = 12.34$ mm.



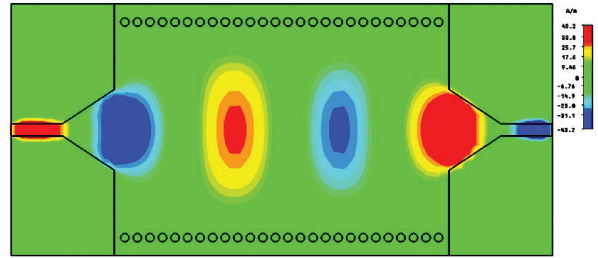
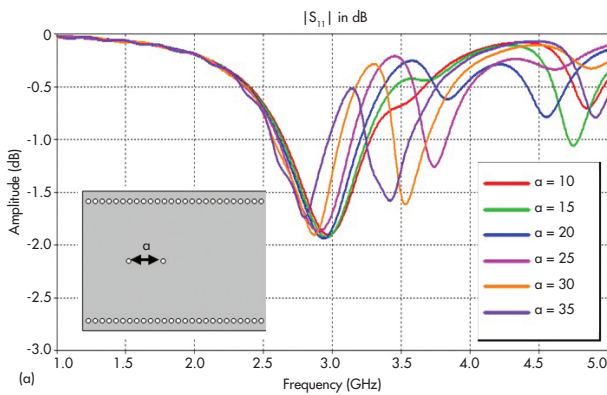
3. These are the return loss and transmission parameters for the filter with parameters of Fig. 2.

engineering (CAE) circuit simulation software. As examples, filters, couplers, and slot antennas have already been made with this technology with good results.⁵⁻¹³ In addition, a number of different methods have been used for the characterization of these components to better understand the performance and behavior of SIW components.¹⁴⁻¹⁹

Filters, of course, are one type of component widely used in modern telecommunications systems, both for processing and providing selectivity among different signals. To explore the capabilities of SIW technology for fabricating filters for a variety of communications applications, a bandpass filter was designed for S-band frequency use based on SIW technology. A commercial circuit simulation software program, CST Microwave Studio from Computer Simulation Technology (www.cst.com),²⁰ was used to simulate the performance of the SIW bandpass filter design and help determine the validity of the design approach.

The cutoff frequency, f_c , for the transverse-electromagnetic (TE) mode of an SIW component is the same as that for a waveguide filled with a dielectric material having relative permittivity of ϵ_r , as computed by Eq. 1:

$$f_c = v/2\pi[(m\pi/a)^2 + (n\pi/b)^2]^{0.5} \quad (1)$$



4. This image represents the electric-field propagation for the SIW conductors.

where:

$$\begin{aligned} m \text{ and } n &= \text{mode numbers,} \\ b &= \text{waveguide dimensions, and} \\ v &= c/(\epsilon_r)^{0.5} \quad (2) \end{aligned}$$

and

v = the relative velocity through the dielectric-filled waveguide,
 c = the speed of light, and
 ϵ_r = the relative permittivity of the dielectric material.

For operation in the transverse-electromagnetic TE₁₀ mode, Eq. 1 can be simplified to the form of Eq. 3:

$$f_c = v/2a \quad (3)$$

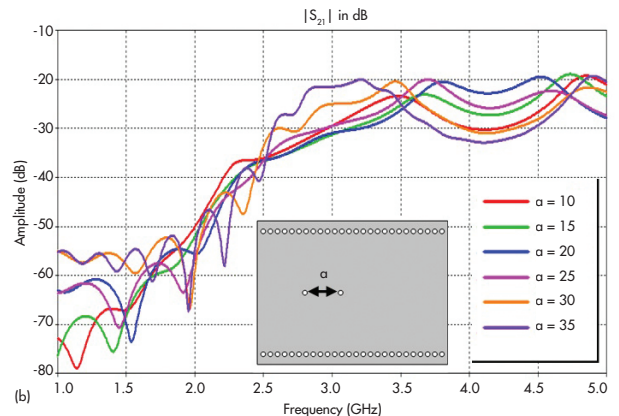
where dimension a equals the width of a rectangular waveguide filled with dielectric material of relative permittivity, ϵ_r , and can be found by means of Eq. 4^{1,2}:

$$a = c/2f_c(\epsilon)^{1.2} \quad (4)$$

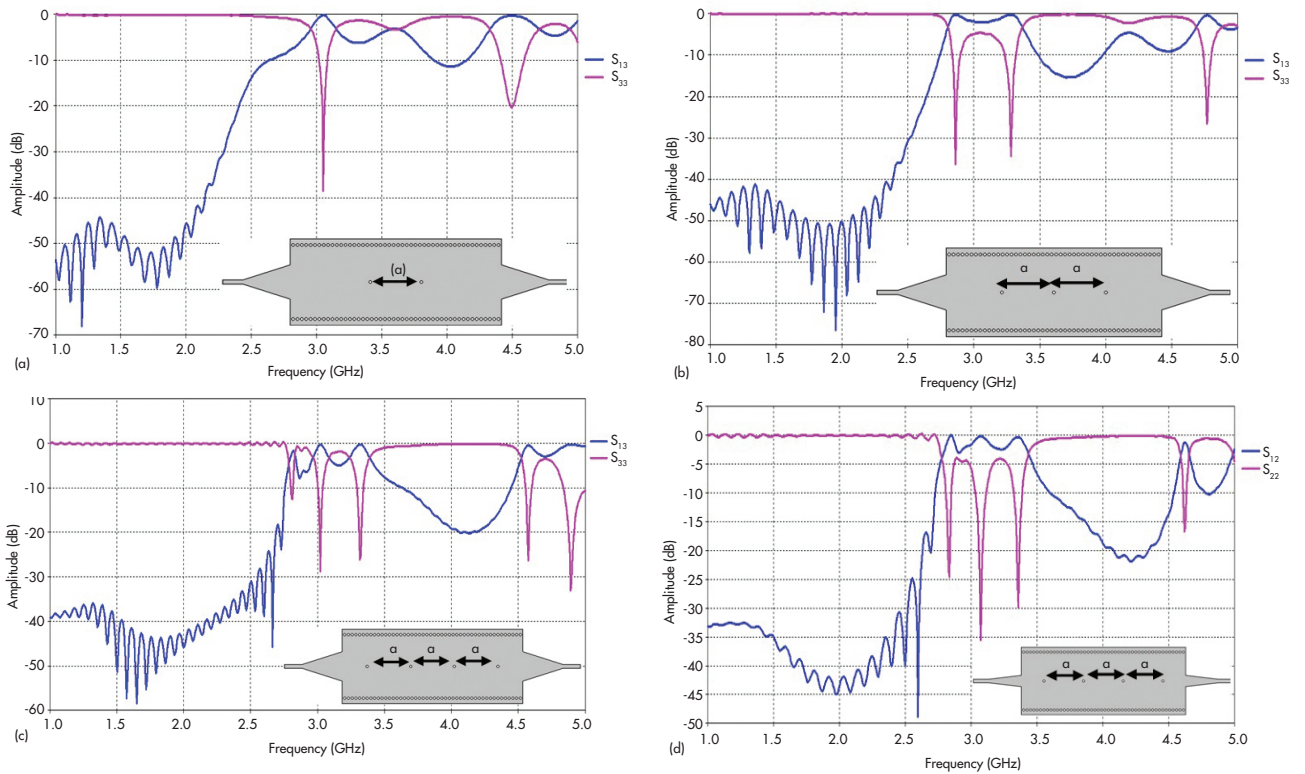
where:

$$a_{\text{SIW}} = a + d^2/0.95p \quad (5)$$

and



5. The plots show the (a) return loss and (b) transmission coefficient characteristics for an SIW filter with transmission coefficients, a , of 10, 15, 20, 25, 30, and 35 mm.



6. The plots show the return loss and transmission coefficient responses for the filter (a) with one cavity, (b) with two cavities, (c) with three cavities, and (d) with three cavities and taper modification, with $a = 35$ mm, $W_2 = 10$ mm, $W_1 = 3.06$ mm, $L_2 = 29.14$ mm, and $L_1 = 12.84$ mm.

d = the diameter of the viaholes, and
 p = the distance between the viaholes.

When designing SIW circuits, a number of conditions are required, including those detailed by Eqs. 6 and 7:

$$d < \lambda_g/5 \quad (6)$$

$$p \leq 2d \quad (7)$$

To adapt a microstrip feedline to an SIW guide, it is necessary to calculate the impedance of the SIW guide according to Eq. 8:

$$Z_{pi} = Z_{TE}(\pi^2 h/8a_s) \quad (8)$$

where Z_{TE} represents the wave impedance for the TE₁₀ mode, as given by Eq. 9^{1,2}:

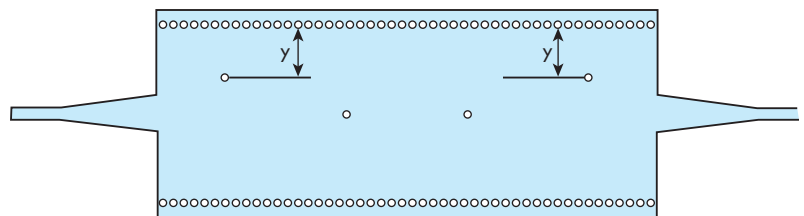
$$Z_{TE} = (\mu/\epsilon)^{0.5} \quad (9)$$

For the design of an SIW filter operating at S-band frequencies (2 to 4 GHz), the design equations were used to calculate the

SIW dimensions. For operation on the TE₁₀ mode, the cutoff frequency, f_c , of 2 GHz was calculated from the effective width of the guide for a dielectric material with relative permittivity, ϵ_r , of 2.17 when measured through the z direction (thickness) of the material at 10 GHz and at a dissipation factor of 0.0013 at 10 GHz.

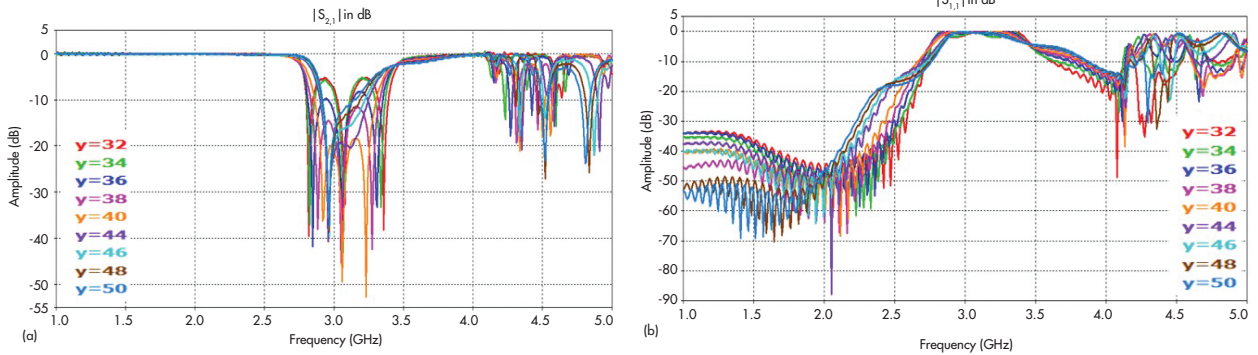
The nonwoven, fiberglass-reinforced polytetrafluoroethylene (PTFE) dielectric material is known commercially as Iso-Clad 917, and is available from Arlon Materials for Electronics (www.arlon-med.com).

After calculating the input impedance of the SIW filter, the next step involved the design of a taper transition for the filter. Figure 2 shows a top view of the SIW waveguide with two tapers operating in the S-band range. Figure 3 presents the performance of this SIW guide with SIW transitions in terms of



7. This simple diagram represents the S-band filter with its modified cavities.

S-Band Filter



8. These plots offer a parametric study for different values of y : (a) return losses and (b) transmission coefficient.

transmission and reflection. Below the design cutoff frequency, f_c , of 2 GHz, minimum transmission and maximum reflection can be seen in Fig. 3.

Beyond 2 GHz, the transmission characteristics improve significantly by means of the taper transition. Several resonant peaks show levels to -41 dB. Figure 4 presents the magnetic-field propagation within the SIW structure at 3 GHz.

For the design of the filter's resonant cavities, it was necessary to add several metal viaholes to the SIW structure. As part of the design process, two viaholes were inserted and the impact of varying distance a between the viaholes was analyzed. Figure

5 offers return losses and transmission coefficients for different values of parameter a for the SIW filter.

According to Fig. 5, good bandpass-filter characteristics were achieved for a distance of 35 mm. As the distance between the viaholes increased, the filter passband and the cutoff frequency moved higher in frequency. To design a practical transition for the SIW filter input, a taper was optimized and integrated into the SIW filter.

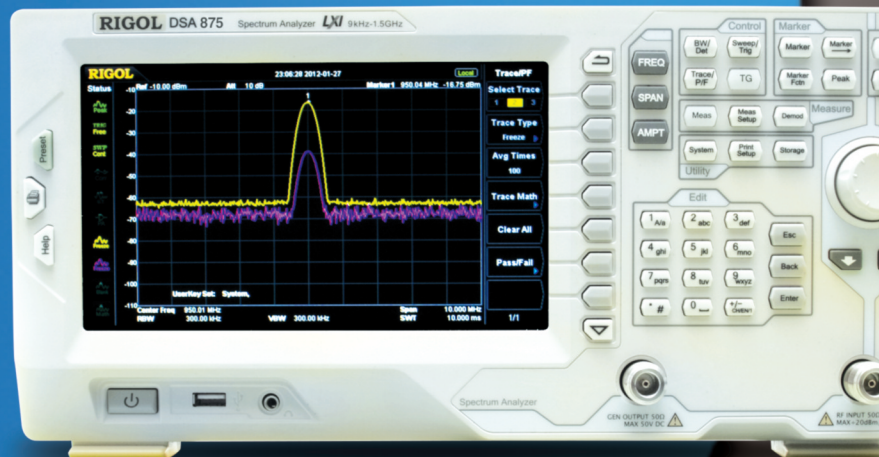
Figure 6 shows the topology of the SIW filter and its transmission and reflection performance from 1 to 5 GHz. Unfortunately, the design exhibits poor rejection in the band from 1 to

DSA800 Series

Spectrum Analyzer

Ideal for WiFi & 2.4 GHz Apps

- 3 Models with Frequencies to 1.5 GHz, 3.2 GHz & 7.5 GHz
- DANL of -161 dBm (typ) Normalized to 1 Hz
- Available Tracking Generator
- EMI and VSWR Packages
- View 3rd Harmonic of 2.4 GHz Wireless Signals
- Models Starting at \$1,295



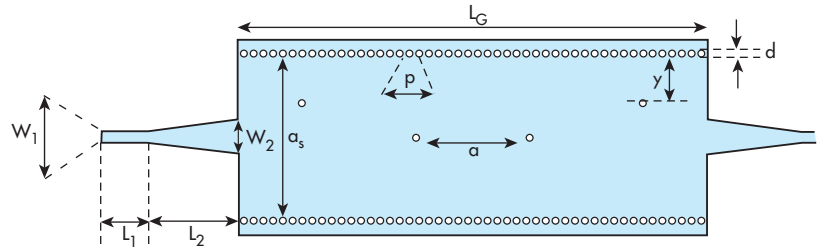
Visit RigolRF.com or call 877-4-RIGOL-1

5 GHz. To improve rejection, it is necessary to increase the number of cavities in the SIW filter design. Figures 6(b), (c), and 6(d) show the results of filter topologies with two and three cavities; the performance of the design with the SIW transition, in terms of transmission and reflection, is plotted in those same figures.

Good rejection was achieved when three cavities were used, although adapting the design to an increased number of cavities required some modifications. To improve the design for use with three cavities, it was thought that the dimensions of the tapers could be adjusted appropriately. Figure 6(d) shows an optimized filter topology after several changes.

The position of the viaholes in the cavities was another structural design parameter that was analyzed for its impact on the SIW filter's performance. The performance of the SIW structure was studied for different positions of the viaholes within the resonant cavities.

Figure 7 shows the filter with its modified cavities, and Fig. 8 offers some of the results of this study. Responses are plotted for return loss and transmission coefficient for different positions of the viaholes. From this analysis, it was found that



9. This is a top view of the final topology of the S-band BPF, with $p = 3$ mm, $d = 2$ mm, $a_s = 51.4$ mm, $a = 35$ mm, $W_2 = 10$ mm, $W_1 = 3.06$ mm, $L_2 = 29.14$, $L_1 = 12.84$ mm, and $y = 10$ mm.

optimum matching conditions occurred at $y = 10$ mm.

Figure 9 shows the final topology of the filter and the responses for that construction, respectively. Fig. 10 (online only) offers curves for the return-loss and transmission-coefficient performance projections from 1 to 5 GHz. A filter bandwidth from 2.75 to 3.40 GHz beyond the S-band passband was recorded, with good impedance matching and acceptable levels of rejection beyond the filter passband.

The filter was fully simulated with CST Microwave Studio. It offers great promise for communications applications at S-band and higher (with reduced dimensions). **IMW**

Note: For Fig. 10 and references, see the online version of this article at www.mwrf.com.

Uncompromised Performance... Unprecedented Value

- Full RF Portfolio
- Spectrum Analyzers, RF Signal Generators & Application Software
- Lower Your Cost of Test



TRY RISK FREE
for 30 days



DSG3000 RF Signal Generator

Oscilloscopes • MSOs • Waveform Generators
RF Test • Precision Measurement